Oceanologia, 67 (2)/2025, 67206
Polish Academy of Sciences
Institute of Oceanology

https://doi.org/10.5697/EUFR9367

Bering Sea climate dynamics forecast by novel multivariate natural hazard assessment method, utilizing self-deconvolution scheme

Alia Ashraf[1], Oleg Gaidai [1,*], Jinlu Sheng[2], Yan Zhu[3], Zirui Liu[1]

Abstract
This case study advocates a generic state-of-the-art multidimensional natural hazards evaluation methodology, applied to windspeeds and wave heights, measured in different offshore locations. Due to complex nonlinear spatiotemporal cross-correlations between different environmental system components and covariates, it is challenging to assess associated environmental risks, utilizing existing reliability techniques. Hence, it is necessary to develop novel multimodal reliability and risk assessment methods for natural hazards prognostics further, given global climate variability. Advocated multivariate risk assessment methodology being particularly suitable for both environmental and offshore/ocean structural systems, which have been either physically measured or numerically simulated over a representative period. National Oceanic and Atmospheric Administration (NOAA) buoys, operating in the central Bering Sea, provided the raw in situ measurements of windspeeds and wave heights, utilized in this case study. A relatively limited amount of underlying data had been analyzed – only 4 months between June and September 2024. The presented multimodal natural hazards prognostics methodology has a generic nature, hence, large amounts of measured data can be analyzed if available. A novel non-parametric deconvolution extrapolation scheme has been utilized to accurately forecast in situ extreme environmental climate dynamics events. System's quasi-stationarity was assumed; otherwise, for nonstationary multidimensional dynamic systems with underlying multivariate trend, this trend has to be identified first, before the advocated reliability methodology to be applied.
Distinct advantage of presented multivariate reliability methodology versus existing ones lies within its ability to overcome "curse of dimensionality", namely ability to treat systems with dimensionality above two.

Keywords
Climate; Dynamic system; Global warming; Stochastics; Windspeed

[1] *Shanghai Ocean University, Shanghai, China*
[2] *Chongqing Jiao Tong University, Chongqing, China*
[3] *Jiangsu University of Science and Technology, Zhenjiang, China*
***Correspondence**: o_gaidai@just.edu.cn (O. Gaidai)

Received: 6 May 2024; **revised:** 3 November 2024; **accepted**: 13 May 2025

1. Introduction

Dynamic complexity and a wide range of random factors, impacting the dynamics of environmental systems, may significantly impair their hazard prognostics (Gaidai et al., 2022a, 2023b; Han et al., 2024b). Direct large-scale Monte Carlo simulations (MCS) or substantial physical measurements may be utilized to evaluate the risks and reliability of spatiotemporal environmental systems, but the costs of computing and measurements are prohibitive in most cases, (Rice, 1944; Madsen et al., 1986; Gaidai et al., 2023c; Qin et al., 2024). To reduce both computational as well as measurement expenses, the authors proposed a novel multivariate reliability approach for both environmental and structural systems risk/hazard assessment, motivated by the aforementioned reasoning (Gaidai et al., 2022b). The most common representation of ocean dynamics is a jointly piecewise-ergodic stochastic/random process. The ocean provides surface smoothness, whereby wind could easily circulate, as opposed to hills, mountains, and forests, which usually block or prevent wind along land. Given the alleged climate change process, it is necessary to expand industrial uses for renewable wind-wave power by exploiting an unexplored portion of the globe's energy assets, particularly in offshore and ocean

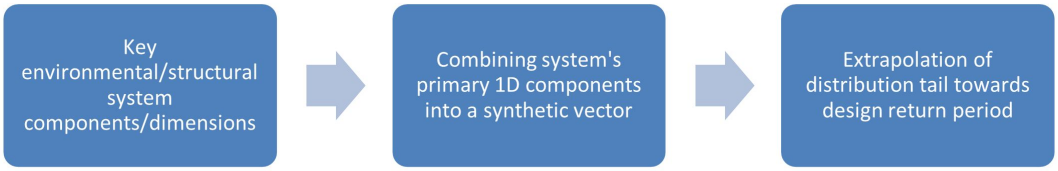

Figure 1. Flow diagram for multidimensional reliability assessment.

locations. This case study advocates a pre-asymptotic non-parametric extrapolation scheme, as opposed to commonly used EVT (Extreme Value Theory) extrapolation techniques, e.g., Gumbel-type, Weibull-type, GP (Generalized Pareto), POT (Peaks Over the Threshold), etc. (Glukhovskii, 1966; Haring et al., 1976; Zhang et al., 2006). Analysis of unusual occurrences of ocean waves, known as freak waves, has to be conducted, however, the number of reliable measurements is still not representative (Jahns and Wheeler, 1973; Tayfun, 1980; Tayfun and Fedele, 2007). For the dynamic coupling between wind and wave dynamics, see Pierson and Marks (1952), Phillips (1957, 1958, 1985), Pierson and Moskowitz (1964), Stansell (2004), Zhang et al. (2019). To minimize operational delays and avoid potential damages to wave energy converters and offshore wind turbines, multivariate generic spatiotemporal structural reliability methods have recently been employed to forecast the frequency and intensity of extreme windspeed and wave-height occurrences (Cook, 2023; Vega-Bayo et al., 2023). One of the main merits of the multivariate Gaidai hazards assessment approach is its ability to examine the reliability of multidimensional stochastic environmental and structural systems with a virtually unlimited number of components or dimensions.

Figure 1 presents a flowchart illustrating the advocated long-term multimodal reliability methodology, which may be applied within various fields of environmental and structural engineering, particularly during the design stage. For issues related to post-processing and uncertainty assessment of measured meteorological data, see Ukhurebor et al. (2020, 2021b), Ukhurebor and Aidonojie Nwankwo and Ukhurebor (2021), Siloko et al. (2021).

Existing environmental and structural reliability methods, except MC-based ones, are limited to bivariate systems, as there is no generalization of EVT to distributions beyond bivariate. Even for bivariate EVT applications, there is reliance on an ad hoc copula assumption, introducing additional inaccuracies. For the environmental contour method, applied to structural reliability of coastal and marine structures, see Ross at al. (2020). For the recently developed SPAR model for bivariate extremes with application to metocean variables, see Mackay at al. (2024). Popular IFORM, ISORM, and hierarchical conditional models are not only limited by 2D dimensionality, but also utilize Rosenblatt transformation, which pre-assumes normality of underlying distributions, which is rarely the case, see Haghayeghi et al. (2018).

To summarize, the primary advantage of the presented multivariate reliability methodology, compared to existing ones, is that systems with dimensionality above two can be treated, while existing reliability methods, except MC-based, like First and Second Order Reliability Methods (FORM, SORM, respectively), can treat only univariate and bivariate systems.

2. Multivariate Gaidai risk assessment approach for dynamic systems of the series type

The spatiotemporal reliability of wind-wave systems is often challenging to estimate using existing risk/hazard assessment techniques. For the majority of complex dynamic environmental and structural systems, reliability evaluation requires expensive either experimental or computational MC (Monte Carlo) efforts. To reduce both measurement and MCS computation costs, this study offers an innovative multimodal approach to risk and hazard evaluation for ocean wind-wave spatiotemporal systems. Short-term windspeeds and wave heights may be described as a dynamic MDOF (Multi-Degree-of-Freedom) system, controlled by in-situ environmental covariates/variables. Let's assume the dynamic system to be jointly homogenous, quasi-stationary, or piecewise ergodic with the system's primary 1D components $(X(t), Y(t), Z(t), ...)$ bring either MCS or measured over a representative period $(0,T)$. Global maxima of all of the system's primary 1D components, recorded across $(0,T)$, to be denoted as $X_T^{\max} = \max_{0\le t\le T} X(t)$, $Y_T^{\max} = \max_{0\le t\le T} Y(t)$, $Z_T^{\max} = \max_{0\le t\le T} Z(t), ...$ The representative value of T is defined as a large $O(1)$ value wrt MDOF system's self-correlation and relaxation time-scales. Let $X_1, ..., X_{N_X}$ denote the local maxima of the $X(t)$ component, recorded in temporally increasing instants: $t_1^X < ... < t_{N_X}^X$. For the rest of the components $Y(t)$, $Z(t), ...$, their local maxima $Y_1, ..., Y_{N_Y}$; $Z_1, ..., Z_{N_Z}$; ... to be defined similarly. Currently, the objective is to estimate the likelihood P_F of environmental/structural systems entering a hazard state.

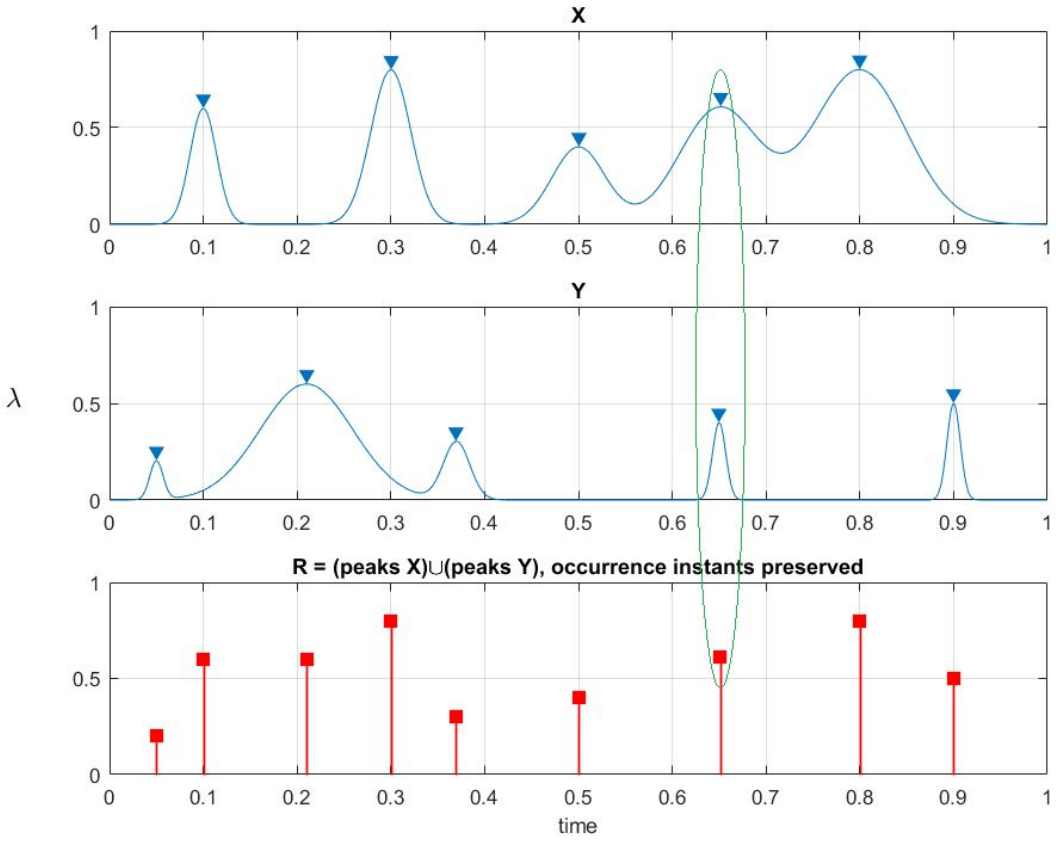

Figure 2. Synthetic vector $\vec{R}$ composed of 2 components, X, Y. Ellipse-marks simultaneous local maxima occurrence originating from X, Y components (Gaidai at al., 2024z).

$$P_F \equiv 1 - P = \text{Prob}(X_T^{\max} > \eta_X \vee Y_T^{\max} > \eta_Y \vee Z_T^{\max} > \eta_Z \vee \dots) \tag{1}$$

with

$$P = \iiint_{(0,\,0,\,0,\dots)}^{(\eta_X,\,\eta_Y,\,\eta_Z,\,\dots)} p_{X_T^{\max},\,Y_T^{\max},\,Z_T^{\max},\,\dots} \times \left(x_T^{\max},\, y_T^{\max},\, z_T^{\max},\, \dots\right) dx_T^{\max} \times dy_T^{\max}\, dz_T^{\max} \dots \tag{2}$$

holding component-wise critical/hazard thresholds/levels η_X, η_Y, ... pre-defined per each system's component, forming merged damage/limit/hazard vector $(\eta_X,\, \eta_Y,\, \dots)$, $\vee$ standing for logical unity-operator, $p_{X_T^{\max},\,Y_T^{\max},\,Z_T^{\max},\,\dots}$ indicating the Joint Probability Density Function (JPDF) of components' global maxima. Direct assessment of high-dimensional JPDF $p_{X_T^{\max},\,Y_T^{\max},\,Z_T^{\max},\,\dots}$ is often impractical due to high NDOF (Number Degrees of Freedom) and underlying dataset limitations. For series-type MDOF its failure/hazard is identified when any of its primary 1D components enter hazard state, i.e., when $X(t)$ surpasses η_X or $Y(t)$ surpasses η_Y, ... Each component's global maxima can be written in discrete form as $X_{N_X}^{\max} = \max\{X_j;\, j = 1, \dots, N_X\} = X_T^{\max}$, $Y_{N_Y}^{\max} = \max\{Y_j;\, j = 1, \dots, N_Y\} = Y_T^{\max}, \dots$. Component's local maxima incidence times $\left[t_1^X < \dots < t_{N_X}^X;\, t_1^Y < \dots < t_{N_Y}^Y;\, t_1^Z < \dots < t_{N_Z}^Z\right]$ can be combined/merged into a single vector $t_1 < \dots < t_N$ preserving temporally monotonic order, holding $t_N = \max\left\{t_{N_X}^X, t_{N_Y}^Y, t_{N_Z}^Z, \dots\right\}$, $N \le N_X + N_Y + N_Z + \dots$. Therefore, t_j denotes instant when certain individual local maxima of one of the components $X(t)$, $Y(t)$, ... occurred. Next, $\vec{R} = (R_1,\, R_2, \dots,\, R_N)$ is defined as a synthetic temporally increasing vector component's local maxima, having incidence times: $t_1 < \dots < t_N$. Figure 2 illustrates formation of the synthetic vector $\vec{R}$ for the case of two 1D components X and Y – in the case when local maxima X_i, Y_j have occurred at the same time instant t_l, $R_l = \max\{X_i,\, Y_j\}$. Simultaneous reduction of failure/damage thresholds for each system's component can be carried out using a scaling parameter $0 < \lambda \le 1$. Scaled hazard/limit vector $\left(\eta_X^\lambda,\, \eta_Y^\lambda, \dots\right)$ consists of η_j^λ, equal to either $\eta_X^\lambda,\, \eta_Y^\lambda \dots$, with $\eta_X^\lambda \equiv \lambda \times \eta_X \equiv \lambda \times \eta_Y, \dots$. The survival probability will then be dependent on λ – i.e., $P(\lambda)$, with

target survival probability being $P \equiv P(1)$. Function $P(\lambda)$ is assumed to be a smooth/differentiable C^1 function of λ, at least in the tail ($\lambda \to 1$)

$$\begin{aligned} P(\lambda) =& \text{Prob}\left\{R_N \le \eta_N^\lambda, \dots, R_1 \le \eta_1^\lambda\right\} = \\ &= \text{Prob}\left\{R_N \le \eta_N^\lambda \mid R_{N-1} \le \eta_{N-1}^\lambda, \dots, R_1 \le \eta_1^\lambda\right\} \\ &\quad \times \text{Prob}\left\{R_{N-1} \le \eta_{N-1}^\lambda, \dots, R_1 \le \eta_1^\lambda\right\} = \\ &= \prod_{j=2}^{N} \text{Prob}\left\{R_j \le \eta_j^\lambda \mid R_{j-1} \le \eta_{j-1}^\lambda, \dots, R_1 \le \eta_1^\lambda\right\} \\ &\quad \times \text{Prob}\left(R_1 \le \eta_1^\lambda\right) \end{aligned} \tag{3}$$

When temporally neighboring R_j is cross-correlated, Eq. (3) can be improved by introducing a conditioning memory level k

$$\begin{aligned} &\text{Prob}\left\{R_j \le \eta_j^\lambda \mid R_{j-1} \le \eta_{j-1}^\lambda, \dots, R_1 \le \eta_1^\lambda\right\} \approx \\ &\approx \text{Prob}\left\{R_j \le \eta_j^\lambda \mid R_{j-1} \le \eta_{j-1}^\lambda, \dots, R_{j-k} \le \eta_{j-k}^\lambda\right\} \end{aligned} \tag{4}$$

with $k < j \le N$. The purpose of these memory approximations is to reduce the amount of intercorrelated local excesses that cluster or cascade. MDOF system is assumed to be quasi-stationary and jointly piecewise ergodic, then probability functions $p_k(\lambda) \coloneqq \text{Prob}\left\{R_j > \eta_j^\lambda \middle| R_{j-1} \le \eta_{j-1}^\lambda, R_{j-k+1} \le \eta_{j-k+1}^\lambda\right\}$ for $j \ge k$ will be independent of j and dependent only on the conditioning memory level k. Following Poisson's assumption, the system's survival probability can be expressed as

$$P_k(\lambda) \approx \exp(-N \times p_k(\lambda)), \quad k \ge 1 \tag{5}$$

holding $N \gg k$. A failure/hazard probability per design is of a low order of magnitude $o(1)$, thus, Eq. (5) is an obvious consequence of Eq. (3), provided $\text{Prob}(R_1 \le \eta_1^\lambda) \approx 1$.

For narrow-band dynamic systems, their component's local maxima, forming vector $\vec{R} = (R_1, R_2, \dots, R_N)$ display clustering/cascading pattern (Gaidai and Xing, 2022; Gaidai et al., 2022c,d,e; Gaidai 2024). Thus, the above-described conditioning memory level scheme can be viewed as a modification of the Poisson assumption (Gaidai et al., 2023f,g; Sun et al., 2023a; Yakimov et al., 2023a,b).

2.1 Self-deconvolution extrapolation scheme

Let's assume the existence of two Independent Identically Distributed (I.I.D.) quasi-stationary processes $X_1(t), X_2(t)$, such that their sum amounts to the underlying process of interest $X(t)$

$$X(t) = X_1(t) + X_2(t) \tag{6}$$

Target PDF p_X is then $p_X = \text{conv}\left(p_{X_1}, p_{X_2}\right)$, with $p_{X_1} = p_{X_2}$ being PDFs of $X_1(t), X_2(t)$. It is then possible to evaluate PDF p_{X_1} using self-deconvolution

$$p_{X_1} = \text{deconv}\,(p_X) \tag{7}$$

Let vector u represent PDF p_{X_1} in discrete form, $u = (u(1), \dots, u(n))$, with $n = \text{length}(u)$. The k-th element of vector w, representing PDF p_X, has length $\text{length}\,(w) = 2n - 1$, and

$$w(k) = \sum_{j=1}^{n} u(j) v(k - j + 1) \tag{8}$$

having

$$\begin{aligned} &w(1) = u(1) \times u(1) \\ &w(2) = u(1) \times u(2) + u(2) \times u(1) \\ &w(3) = u(1) \times u(3) + u(2) \times u(2) + u(3) \times u(1) \\ &w(n) = u(1) \times u(n) + u(2) \times u(n-1) + \dots + u(n) \times u(1) \\ &w(2n-1) = u(n) \times u(n) \end{aligned} \tag{9}$$

Eq. (9) provides deficient versions of w as the running index moves from $n+1$ to $2n-1$. As a result, vector w covers double the original PDF support domain $(2n-1) \times \Delta x \approx 2n \times \Delta x = 2X_L$, which means that the PDF support's length has doubled, compared with the original u vector PDF's support length of $n \times \Delta x = X_L$, with Δx representing PDF's bin width. Starting with the vector's u first element, $u(1) = \sqrt{w(1)}$, deconvolution moves on to the 2nd, $u(2) = \frac{w(2)}{2u(1)}$, and finally reaches the final vector's u element, $u(n)$. The extended range $(X_L,\ 2X_L)$ can be covered by linear extrapolation of the PDF tail of p_{X_1}. Discrete/empirical PDFs are not sufficiently C^1 smooth/regular, necessitating the smoothing of the PDF tail. 4-variables Weibull-type extrapolation scheme was utilized for the extrapolation of the PDF tail, provided the PDF tail is convex/concave. The following f_X may represent both PDF p_X as well as supplementary $\overline{\text{CDF}}$ (i.e., Cumulative Distribution Function), namely $\overline{\text{CDF}} \equiv 1 - \text{CDF}$. The subsequent scaling approach was developed to avoid negative components within the deconvoluted u vector. First, let one define the least positive value f_L, present within the PDF/ $\overline{\text{CDF}}$ f_X tail. Second, scaling and linear correction are to be performed on the decimal logarithmic scale

$$g_X = \mu\left(\log_{10}(f_X) - \log_{10}(f_L)\right) + \log_{10}(f_L) \tag{10}$$

with $g_X(x)$ being $\log_{10}$ – a scaled form of an empirical PDF/ $\overline{\text{CDF}}$ f_X, provided a suitable scaling parameter $\mu < 1$.

Extrapolated PDF/ $\overline{\text{CDF}}$ distribution can be obtained via convolution $\tilde{f}_X = \text{conv}\left(f_{X_1}, f_{X_1}\right)$. To restore the original distribution scale, inverse linear scaling following Eq. (10) has to be carried out.

3. Results for the quadrivariate system

The efficiency of the spatiotemporal multivariate Gaidai risks assessment approach is demonstrated in this section by utilizing coherently measured wind speed and wave heights, obtained from NOAA buoys in the Bering Sea. Measured wind speeds and corresponding wave heights were averaged over 10-minute periods. Wind-wave spatiotemporal dynamics is recognized as a multifaceted, extremely nonlinear, cross-correlated dynamic system that is challenging to forecast. For marine and offshore structures functioning in a designated offshore region of significance and affected by extreme offshore conditions, an environmental method risk/hazard evaluation is essential. For this study, two NOAA offshore wind and wave observation locations were selected:

I. Station 46035 (LLNR 1198) – CENTRAL BERING SEA – 310 NM North of Adak, AK Owned and maintained by National Data Buoy Center 57.034 N 177.468 W (57°2′1′′N 177°28′4′′W)

II. Station 46072 (LLNR 27510) – CENTRAL ALEUTIANS 230 NM SW Dutch Harbor Owned and maintained by National Data Buoy Center 51.645 N 172.145 W (51°38′42′′N 172°8′42′′W)

Two stations yielded a 4D (quadrivariate) system $X = (X, Y, W, Z)$, consisting of synchronous measurements of

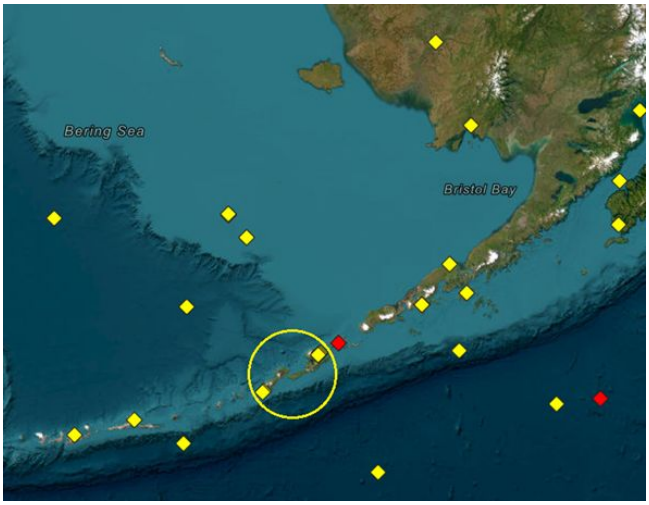

Figure 3. The circle indicates two chosen NOAA windspeed observation localities near the Bering Sea. Source: (National Oceanic and Atmospheric Administration, NOAA (2024)).

Figure 4. NOAA buoy. Source: (National Oceanic and Atmospheric Administration, NOAA (2024)).

corresponding 2 windspeeds and wave heights. Critical/hazard thresholds/limits η_X, η_Y, ... for each of the four system components had been set to be equal to respective global maxima, recorded over the entire observational period, i.e., 4 months between June and September 2024. Figure 3 displays the North Pacific NOAA buoy stations, with a circle marking the area of interest.

A NOAA data buoy with sensors to detect and acquire meteorological data from the ocean is shown in Figure 4. Collected data is converted into an electrical signal that could be maintained within the outboard data module or transferred to land. Technical specs of the 3-meter-high NOAA buoy and positional characteristics of its sensor are as follows:

I. The location's altitude was measured in MSL (i.e., Mean Sea Level). The temperature of the atmosphere was 3.4 meters above MSL.

II. The anemometer was 3.8 meters above MSL.

III. Barometer altitude: 2.4 meters above MSL.

All 4 measured wind-wave time-series had been non-dimensionalized resulting in uniform failure/hazard limits all equal to 1. All component local maxima were merged into synthetic vector $\vec{R} = (\max\{X_1, Y_1, W_1, Z_1\}, \ldots, \max\{X_N, Y_N, W_N, Z_N\})$. Figure 5 presents full-scale measurements in the form of a 2D configuration space. Figure 6 illustrates a synthetic non-dimensional $\vec{R}$ vector that exhibits monthly fluctuations.

Figures 5 and 6 illustrate the process of coalescing distinct system's inter-correlated components (windspeed and wave height) into one synthetic nondimensional vector $\vec{R}$. Deconvolution of the $\overline{\text{CDF}}$ tail was utilized to extrapolate the distribution tail towards the target/design hazard

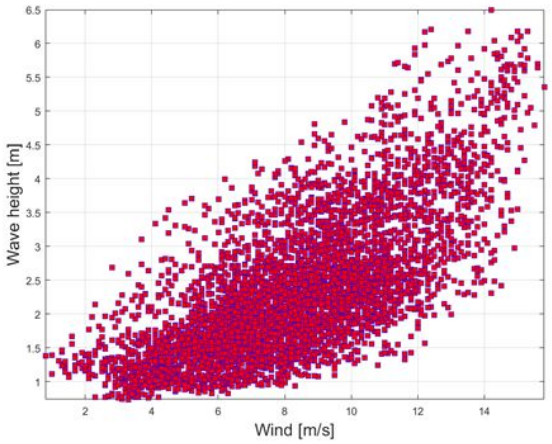

Figure 5. Full scale windspeed and wave-height data.

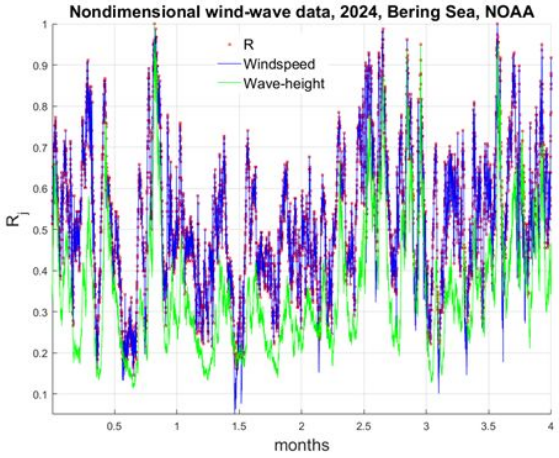

Figure 6. Nondimensional synthetic vector $\vec{R}$.

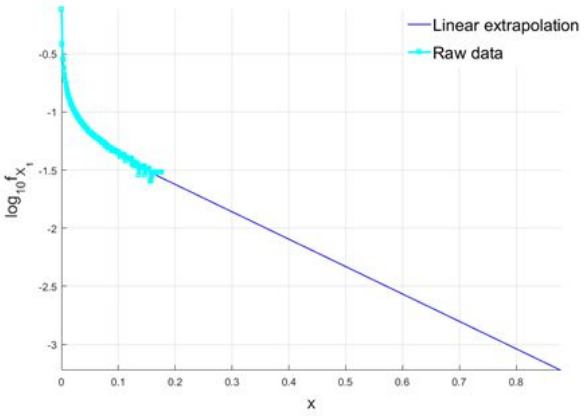

Figure 7. Linear extrapolation for PDF $[p]_X$, see Eq. (7)

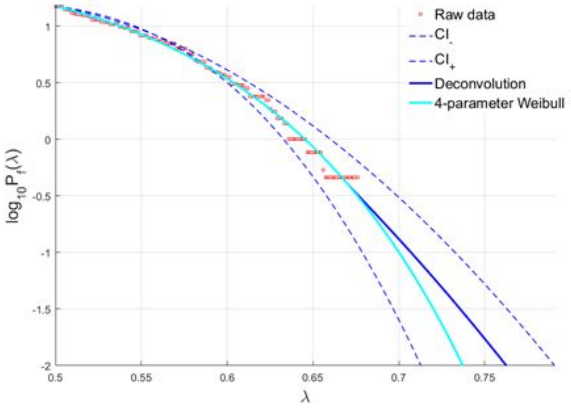

Figure 8. 4-parameter Weibull extrapolation (cyan), raw dataset (red), and extrapolation by deconvolution scheme (dark blue). 95% CIs indicated with 2 dashed lines.

probability level. Since the synthetic vector $\vec{R}$ was composed of entirely distinct components (i.e., windspeeds and wave heights), it should be underlined that there is no physical meaning in the vector $\vec{R}$ itself. Each 10$^{\text{th}}$ data point obtained from «longer/full» windspeed and wave-height dataset had been retained to construct a «shorter/reduced» dataset version. Based on the «shorter/reduced» dataset, the forecasted hazard λ-level, having a 1-year return period, had been found to lie within the 95% CI (confidence interval), predicted using «longer/full» windspeed and wave height dataset. Figure 7 presents linear extrapolation for the deconvoluted PDF p_X, see Eq. (7). Figure 8 presents the decimal log scale CDF f_X tail extrapolating for the «longer/full» dataset using a 4-parameter Weibull and non-parametric deconvolution scheme.

Figures 7 and 8 illustrate the self-deconvolution extrapolation scheme in action, i.e., applied to a specific bivariate windspeed and wave-height dataset. Note that extrapolation is performed in 1D space, i.e., for synthetic nondimensional vector $\vec{R}$.

Figure 8 illustrates the non-parametric deconvolution scheme's benefit over the 4-parameter Weibull-fit, as the latter scheme predicts a less conservative hazard λ level. The cut-on value $\lambda_{\text{cut on}} = 0.5$ had been selected in Figure 8 (Gaidai et al., 2023a,b,d,e,f; 2024e,i,k,u). Another key benefit of the deconvolution extrapolation scheme lies within its non-parametric nature, which assures increasing numerical stability, compared with parametric extrapolation schemes (Gaidai et al., 2024a,d,f).

The Poincare plot forms the basis for the widely used SODP (Second-Order Difference Plot). SODP may underline intrinsic statistical dependencies contained within consecutive differences, derived from raw/unfiltered data.

The underlying dataset's pattern may be compared to that of other relevant datasets, using the SODP plot, presented in Figure 9. Various AI (Artificial Intelligence) pattern identification techniques can be applied, e.g., entropy scheme (Yayık, 2019; Gaidai et al., 2024t). Other schemes like MCP (Measure-Correlate-Predict) can be utilized to gain additional insights into an underlying data structure (Ishihara and Yamaguchi, 2015).

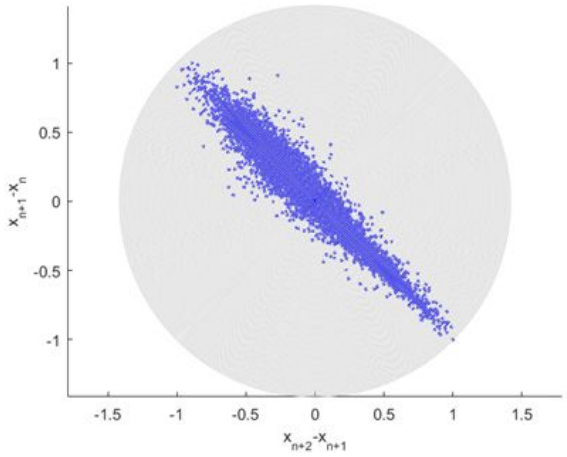

Figure 9. SODP plot for raw measured windspeed and wave-height data.

Note that the multivariate Gaidai risks evaluation approach is mathematically exact and thus may incorporate any extrapolation scheme (Gaidai et al., 2024c,g,h,i,j,l; Han et al., 2024a). Forecast errors may arise either from the chosen extrapolation scheme or from the underlying dataset itself (Gaidai et al., 2024a,m,o,p,q,r,s,t).

Note that separate correlation analysis is not required, as all underlying multivariate data, along with intrinsic component-wise correlations, were embedded into the synthetic vector $\vec{R} \triangleq R(t)$ without any data and information loss. The de-clustering procedure, given by Eq. (3) ensures that temporal and component-wise correlations are accounted for.

4. Discussion

The practical advantages of the suggested generic multimodal Gaidai risk evaluation approach are briefly outlined in Table 1. In summary, the multimodal Gaidai risk assessment approach allows for virtually infinite NDOF, whereas existing reliability techniques are mostly restricted to 1D and 2D dynamic systems. Another distinct advantage of the proposed reliability method lies in its ability to account for memory effects and perform multivariate data declustering.

The system's joint quasi-stationarity assumption may be viewed as a constraint on the proposed multivariate reliability strategy. However, in cases when the underlying multivariate trend can be identified and forecasted, the multimodal Gaidai hazard assessment methodology can well be applied, provided damage/limit/hazard vector $\eta = (\eta_X, \eta_Y, ...)$ is made time-dependent, i.e., $\eta(t)$, (Gaidai, 2025a,b).

Non-parametric self-deconvolution scheme has an advantage over parametric schemes, as it possesses increased numerical stability, moreover, it does not rely on the asymptotic EVT assumption. In this case study non-parametric self-deconvolution scheme had been utilized, however, any suitable extrapolation scheme can be plugged in.

Table 1. Characteristics of the multimodal Gaidai risk analysis approach.

	Multimodal Gaidai hazard assessment method	The present techniques for evaluating risk in univariate or bivariate
Multivariate nonlinear wind-wave system analysis	NDOF = ∞D	NDOF ≤ 2D
Possibility of incorporating wind-wave system trends	Full	Partial-to-full
Extrapolation scheme	Non-parametric	Parametric

5. Conclusions

The presented case study benchmarked a novel multimodal Gaidai reliability approach, utilizing a raw wind-wave dataset, measured in the Bering Sea. In situ climate dynamics was modelled as a quadrivariate dynamic system. The primary benefit of the suggested multimodal reliability approach lies in its capacity to forecast risks of natural hazards related to multivariate environmental and structural systems. Windspeeds and wave heights, measured by NOAA buoys in the Bering Sea in the year 2024 been analyzed. Two distinct extrapolation schemes were utilized, namely, parametric Weibull and non-parametric deconvolution, resulting in environmental wind-wave system hazard risk assessment. The proposed multimodal Gaidai reliability approach's theoretical basis has been thoroughly explained. The development of accurate, conservative, yet reliable natural hazard prognostic methods that can utilize even limited underlying raw datasets is necessary for the design of offshore, ocean, and marine structures. The presented case study's primary objective was to demonstrate the efficiency of the state-of-the-art, generic spatiotemporal reliability approach to climate dynamics. Hazard risks of a wide range of environmental and structural systems can be analyzed with the help of the advocated multimodal Gaidai reliability approach, as it is of a generic nature and is not restricted by the presented wind-wave dynamics case study.

As this is an illustrative case study, it aims to demonstrate the capabilities of the novel multivariate reliability method. Extensive references are provided, covering a wider range of applications of the advocated novel reliability methodology. Other geographical locations can be added, however, then this case study will not be constrained to the Bering Sea area of interest only. Authors have chosen the latest measured data from the year 2024 to provide the latest, up-to-date analysis, as utilizing previous years would introduce annual trend-related bias. As

was previously mentioned, in case of the underlying trend, it has to be identified first, however, trend forecast was not covered in this case study.

Acknowledgements

Author contributions: all authors had contributed equally. Data availability: Data will be available on request from the corresponding author.

Conflict of interest

None declared.

References

Cook, N.J., 2023. *Reliability of Extreme Wind Speeds Predicted by Extreme-Value Analysis*, Meteorology 2 (3), 344–367. https://doi.org/10.3390/meteorology2030021

Ditlevsen, O., Madsen, H.O., 1996. *Structural reliability methods*. John Wiley & Sons, Inc., Chichester (UK).

Gaidai, O., 2024. *Pacific Ocean Windspeeds Prediction by Gaidai Multivariate Risks Evaluation Method, Utilizing Self-Deconvolution*, ASME Open J. Eng. 3, 031025. https://doi.org/10.1115/1.4066682

Gaidai, O., 2025a. *Israel COVID-19 data verification by multimodal Gaidai reliability method*. ASME J. Eng. Sci. Med. Diagn. Ther. JESMDT-25-1003. https://doi.org/10.1115/1.4068499

Gaidai, O., 2025b. *Emotional excess prognostics by multimodal Gaidai reliability methodology, using thorax respiration signal*, ASME J. Eng. Sci. Med. Diagn. Ther. JESMDT-24-1103. https://doi.org/10.1115/1.4068500

Gaidai, O., Ashraf, A., Cao, Y., Sheng, J., Zhu, Y., Liu, Z., 2024a. *Lifetime assessment of semi-submersible wind turbines by Gaidai risk evaluation method*. J. Mater. Sci.: Mater. Eng. 19 (2). https://doi.org/10.1186/s40712-024-00142-2

Gaidai, O., Ashraf, A., Cao, Y., Sheng J., Li, H., Liu, Z., Zhu, Y., 2024b, *Gaidai multimodal risk evaluation methodology based on cargo vessel onboard measurements, given structural damage accumulation*. Discover Oceans 1 (28). https://doi.org/10.1007/s44289-024-00030-9

Gaidai, O., Ashraf, A., Sheng, J. et al., 2024c. *Onboard multivariate hazard assessment for UIKKU chemical tanker by Gaidai reliability method*. Discov. Oceans 1 (26). https://doi.org/10.1007/s44289-024-00027-4

Gaidai, O., Cao, Y., Ashraf, A., Sheng, J., Zhu, Y., Liu, Z., 2024d, *FPSO/LNG hawser system lifetime assessment by multimodal Gaidai risk assessment method*. Energy Inform. 7 (51). https://doi.org/10.1186/s42162-024-00350-2

Gaidai, O., Cao, Y., Li, H., Liu, Z., Ashraf, A., Zhu, Y., Sheng, J., 2024e, *Multivariate Gaidai hazard assessment method in combination with deconvolution scheme to predict extreme wave heights*. Res. Eng. 22, 102326. https://doi.org/10.1016/j.rineng.2024.102326

Gaidai, O., Cao, Y., Wang, F., Zhu, Y., 2024f. *Applying the multivariate Gaidai reliability method in combination with an efficient deconvolution scheme to prediction of extreme ocean wave heights*. Mar. Syst. Ocean Tech. 19, 165–178. https://doi.org/10.1007/s40868-024-00145-w

Gaidai, O., Cao, Y., Xing, Y., Wang, J., 2023a. *Piezoelectric Energy Harvester Response Statistics*. Micromachines 14 (2), 271. https://doi.org/10.3390/mi14020271

Gaidai, O., Cao, Y., Zhu, Y., Zhang, F., Li, H., 2024g. *Multivariate Risk Assessment for Offshore Jacket Platforms by Gaidai Reliability Method*. J. Mar. Sci. Appl. 24, 428–436. https://doi.org/10.1007/s11804-024-00542-y

Gaidai, O., Cao, Y., Zhu, Y., Zhang, F., Liu, Z., Wang, K., 2024h. *Limit hypersurface state of the art multimodal Gaidai risk evaluation approach for offshore Jacket*. Mech. Based Des. Struc. 53, 1–16. https://doi.org/10.1080/15397734.2024.2379523

Gaidai, O., He, S., Ashraf, A., Sheng, J., Zhu, Y., 2024i. *Greenland Wind-Wave Bivariate Dynamics by Gaidai Natural Hazard Spatiotemporal Evaluation Approach*, Atmosphere 15 (11), 1357. https://doi.org/10.3390/atmos15111357

Gaidai, O., He, S., Wang, F., 2024j. *State-of-the-art nonstationary hypersurface damage assessment approach for energy harvesters*. Renew. Energ. 121824. https://doi.org/10.1016/j.renene.2024.121824

Gaidai, O., Li, H., Cao, Y., Ashraf, A., Zhu, Y., Liu, Z., 2024k. *Shuttle tanker operational reliability study by multimodal Gaidai risk assessment method, utilizing deconvolution scheme*. Transport. Res. Interdiscip. 26, 101194. https://doi.org/10.1016/j.trip.2024.101194

Gaidai, O., Li, H., Cao, Y., Liu, Z., Zhu, Y., Sheng, J., 2024l. *Wind turbine gearbox reliability verification by multivariate Gaidai reliability method*. Results Eng. 23. https://doi.org/10.1016/j.rineng.2024.102689

Gaidai O., Liu Z., Cao Y., Zhang F., Zhu Y., Sheng J., 2024m. *Limit hypersurface state-of-the-art damage assessment approach for a galloping energy harvester, accounting for memory effects*. J. Vib. Control https://doi.org/10.1177/10775463241279993

Gaidai, O., Sheng, J., Cao, Y. Zhu, Y., Wang, K., Liu, Z., 2024n. *Limit hypersurface state of art Gaidai risk assessment approach for oil tankers Arctic operational safety*. J. Ocean Eng. Mar. Energ. 10, 351–364. https://doi.org/10.1007/s40722-024-00316-2

Gaidai, O., Sheng, J., Cao, Y., Zhang, F., Zhu, Y., Liu, Z., 2024o. Gaidaimultivariateriskassessmentmethodforcargoshipdynamics. Urban, Planning and Transport Research.

12, 1.
https://doi.org/10.1080/21650020.2024.2327362

Gaidai, O., Sheng, J., Cao, Y., Zhang, F., Zhu, Y., Liu, Z., 2024p. *Design of floating wind turbine gearboxes using Gaidai risk assessment method*. Procedia CIRP, 128, 120–125. https://doi.org/10.1016/j.procir.2024.06.011

Gaidai, O., Sheng, J., Cao, Y., Zhu, Y., Liu, Z., 2024q. *Evaluating Areal Windspeeds and Wave Heights by Gaidai Risk Evaluation Method*. Nat. Hazards Rev. 25 (4). https://doi:10.1061/NHREFO.NHENG-2184

Gaidai, O., Sun, J. Cao, Y., 2024r. *FPSO/FLNG mooring system evaluation by Gaidai reliability method*. J. Mar. Sci. Tech.-Japan. 29, 546–555. https://doi.org/10.1007/s00773-024-01001-7

Gaidai, O., Wang, F., Wu, Y., Xing Y., Rivera Medina, A., Wang, J., 2022a. *Offshore renewable energy site correlated wind-wave statistics*. Probabilistic Engineering Mechanics, 68. https://doi.org/10.1016/j.probengmech.2022.103207

Gaidai, O., Wang, F., Cao, Y. et al., 2024s. *4400 TEU cargo ship dynamic analysis by Gaidai reliability method*. J. Shipp. Trd. 9, 1. https://doi.org/10.1186/s41072-023-00159-4

Gaidai, O., Wang, F., Yakimov, V., Sun, J., Balakrishna, R., 2023b, *Lifetime assessment for riser systems*. Green Tech. Res. Sustain. 3. https://doi.org/10.1007/s44173-023-00013-7

Gaidai, O., Wang, K., Wang, F., Xing, Y., Yan, P., 2022b. *Cargo ship aft panel stresses prediction by deconvolution*. Mar. Struct. 88. https://doi.org/10.1016/j.marstruc.2022.103359

Gaidai, O., Xing, Y., 2022. *Novel reliability method validation for offshore structural dynamic response*. Ocean. 266 (5). https://doi.org/10.1016/j.oceaneng.2022.113016

Gaidai, O., Xing, Y., Xu, X., 2023c, *Novel methods for coupled prediction of extreme windspeeds and wave heights*. Sci. Rep. UK. 13, 1119. https://doi.org/10.1038/s41598-023-28136-8

Gaidai, O., Xu, J., Hu, Q., Xing, Y., Zhang, F., 2022. *Offshore tethered platform springing response statistics*. Sci. Rep. UK. 12. http://www.nature.com/articles/s41598-022-25806-x

Gaidai, O., Xu, J., Xing, Y., Hu, Q., Storhaug, G., Xu, X., Sun, J., 2022d. *Cargo vessel coupled deck panel stresses reliability study*. Ocean Eng. 268, 113318. https://doi.org/10.1016/j.oceaneng.2022.113318

Gaidai, O., Xu, J., Yakimov, V., Wang, F., 2023d. *Liquid carbon storage tanker disaster resilience , Environment Systems and Decisions*. https://doi.org/10.1007/s10669-023-09922-1

Gaidai, O., Xu, J., Yan, P., Xing, Y., Zhang, F., Wu, Y., 2022e. *Novel methods for windspeeds prediction across multiple locations. Sci. Rep. UK, 12, 19614.* https://doi.org/10.1038/s41598-022-24061-4

Gaidai, O., Yakimov, V., Wang, F., Cao, Y., 2024t. *Gaidai Multivariate Risk assessment Method for Energy Harvester Operational Safety, Given Manufacturing Imperfections*. Int. Precis Eng. Man. 25, 1011–1025. https://doi.org/10.1007/s12541-024-00977-x

Gaidai, O., Yakimov, V., Wang, F., Hu, Q., Storhaug, G., 2023e. *Lifetime assessment for container vessels*. Appl. Ocean. Res. https://doi:10.1016/j.apor.2023.103708

Gaidai, O., Yakimov, V., Wang, F., Sun, J., Wang, K., 2024u. *Bivariate reliability analysis for floating wind turbines*. Int. J. Low-Carbon Tec. Vol. 19, 55–64. https://doi.org/10.1093/ijlct/ctad108

Gaidai, O., Yakimov, V., Wang, F., Zhang, F., 2023f. *Safety design study for energy harvesters*. Sustainable Energy Research, Vol. 10 (1). https://doi.org/10.1186/s40807-023-00085-w

Gaidai, O., Yakimov, V., Wang, F., Zhang, F., Balakrishna, R. 2023g. *Floating wind turbines structural details fatigue life assessmen*. Sci. Rep. UK 13 (1). https://doi:10.1038/s41598-023-43554-4

Glukhovskii, B., 1966. *Investigation of sea wind waves*. Gidrometeoizdat (in Russian).

Haghayeghi, Z., Ketabdari, M., 2018. *A long-term joint probability model for metocean circular and linear characteristics*. Appl. Ocean Res. 75, 143–152. https://doi.org/10.1016/j.apor.2018.03.009

Han, C., Gaidai, O., El-Wazery, M., He, S., Ashraf, A., Sheng, J., Zhu, Y., 2024a. *Bivariate validation of the Gaidai natural hazard evaluation method for climate dynamics*. Ocean Eng. 313 (3), 119630. https://doi.org/10.1016/j.oceaneng.2024.119630

Han, C., Gaidai, O., Zhu, Y., Ashraf, A., Qin, P., Sheng, J., 2024b. *Multivariate Gaidai reliability methodology for marine riser dynamics in the Red Sea with memory effects included*. Ocean Eng. 313 (2), 119437. https://doi.org/10.1016/j.oceaneng.2024.119437

Haring, R., Osborne, A., Spencer, L., 1976. *Extreme wave parameters based on continental shelf storm wave records*. Proc. 15th Int. Conf. Coastal Engineering, Honolulu, HI , 151–170.

Ishihara, T., Yamaguchi, A., 2015. *Prediction of the extreme windspeed in the mixed climate region by using Monte Carlo simulation and measure-correlate-predict method*. Wind Energ. 18 (1), 171–186. https://doi.org/10.1002/we.1693

Jahns, H., Wheeler, J., 1973. *Long-term wave probabilities based on hindcasting of severe storms*. J. Petrol. Technol. 25, 473–486.

Mackay, E., Murphy-Barltrop, C., Jonathan, P., 2024. *The SPAR model: a new paradigm for multivariate extremes. application to joint distributions of metocean variables*. Proc. ASME 2024 43rd Int. Conf., Ocean, Offshore & Arctic Eng. OMAE 2024, June 9–14, 2024, Singapore

EXPO.
https://ore.exeter.ac.uk/repository/handle/10871/136413

Madsen, H.O., Krenk, S., Lind, N.C., 1986. *Methods of structural safety*. Prentice-Hall Inc., Englewood Cliffs.

NAG Toolbox for Matlab. NAG Ltd., Oxford, UK.

NOAA, 2024. *National Oceanic and Atmospheric Administration*.
https://www.ndbc.noaa.gov

Nwankwo, W., Ukhurebor, K., 2021. *Big data analytics: A single window IoT-enabled climate variability system for all-year-round vegetable cultivation*. IOP Conf. Ser.: Earth Environ. Sci. 655, 012030.
https://doi10.1088/1755-1315/655/1/012030

Phillips, O., 1957. *On the generation of waves by turbulent wind*. J. Fluid Mech. 2, 417–445.

Phillips, O., 1958. *The equilibrium range in the spectrum of wind-generated waves*. J. Fluid. Mech. 4, 426–434.

Phillips, O., 1985. *Spectral and statistical properties of the equilibrium range in wind-generated gravity waves*. J. Fluid. Mech. 156, 505–531.

Pierson, W.J., Marks, W., 1952. *The power spectrum analysis of ocean-wave records*. T. Am. Geophys. Union 33, 834–844.

Pierson, W.J., Moskowitz, L., 1964. *A proposed spectral form for fully developed wind seas based on the similarity theory of S. A. Kitaigorodskii*. J. Geophys. Res. 69, 5181–5190.

Qin, P., Gaidai, O., Sheng, J., Zhu, Y., Li, H., Cao, Y., Liu, Z., 2024. *Multivariate risk assessment for offshore structures by Gaidai risk evaluation method under an accumulation of fatigue damage, utilizing novel deconvolution scheme*. Structures, 70, 107691.
https://doi.org/10.1016/j.istruc.2024.107691

Rice, S.O., 1944. *Mathematical analysis of random noise*. Bell System Tech. J. 23, 282–332.

Ross, E., Astrup, O., Bitner-Gregersen, E., Bunn, N., Feld, G., Gouldby, B., Huseby, A., Liu, Y., Randell, D., Vanem, E., Jonathan, P., 2020. *On environmental contours for marine and coastal design*. Ocean Eng. 195, 106194.
https://doi.org/10.1016/j.oceaneng.2019.106194

Siloko, I., Ukhurebor, K., Siloko, E., Enoyoze, E., Bobadoye, A., Ishiekwene, C., Uddin, O., Nwankwo, W., 2021. *Effects of some meteorological variables on cassava production in Edo State, Nigeria via density estimation*. Sci. Afr. 13, e00852.
https://doi.org/10.1016/j.sciaf.2021.e00852

Stansell, P., 2004. *Distribution of freak wave heights measured in the North Sea*. Appl. Ocean Res. 26, 35–48.

Sun, J., Gaidai, O., Wang, F., Yakimov, V., 2023a. *Gaidai reliability method for fixed offshore structures*. J. Braz. Soc. Mech. Sci. Eng. 46, 27.
https://doi.org/10.1007/s40430-023-04607-x

Sun, J., Gaidai, O., Xing, Y., Wang, F., Liu, Z., 2023b. *On safe offshore energy exploration in the Gulf of Eilat*. Qual. Reliab. Eng. Int. 39 (7), 2957–2966.
https://doi.org/10.1002/qre.3402

Tayfun, M.A., 1980. *Narrow-band nonlinear sea waves*. J. Geophys. Res. 85, 1548–1552.

Tayfun, M.A., Fedele, F., 2007. *Wave-height distributions and nonlinear effects*. Ocean Eng. 34, 1631–1649.

Ukhurebor, K., Azi, S., Aigbe, U., Onyancha, R., Emegha, J., 2020. *Analyzing the uncertainties between reanalysis meteorological data and ground measured meteorological data*. Measurement, 165, 108110.
https://doi.org/10.1016/j.measurement.2020.108110

Ukhurebor, K.E., Aidonojie, P.A., 2021a. *The influence of climate change on food innovation technology: review on topical developments and legal framework*. Agric & Food Secur 10, 50.
https://doi.org/10.1186/s40066-021-00327-4

Ukhurebor, K., Singh, K., Nayak, V., Eghonghon, G., 2021b. *Influence of the SARS-CoV-2 pandemic: a review from the climate change perspective*. Environ. Sci.-Proc. Imp. 8.
https://doi.org/10.1039/D1EM00154J

Vega-Bayo, M., Pérez-Aracil, J., Prieto-Godino, L., Salcedo-Sanz, S., 2023. *Improving the prediction of extreme wind speed events with generative data augmentation techniques*. Renew Energ. 221, 119769.
https://doi.org/10.1016/j.renene.2023.119769

Yakimov, V., Gaidai, O., Wang, F., Wang, K., 2023a. *Arctic naval launch and recovery operations, under ice impact interactions*. Appl. Eng. Sci. 15, 100146.
https://doi.org/10.1016/j.apples.2023.100146

Yakimov, V., Gaidai, O., Wang, F., Xu, X., Niu, Y., Wang, K., 2023b. *Fatigue assessment for FPSO hawsers*. Int. J. Nav. Arch. Ocean. 15, 100540.
https://doi.org/10.1016/j.ijnaoe.2023.100540

Yayık, A., Kutlu, Y., Altan, G., 2019. *Regularized HessELM and Inclined Entropy Measurement for Congestive Heart Failure Prediction*. Cornell University.
https://arxiv.org/abs/1907.05888

Zhang, H., Reynolds, R. Bates, J., 2006. *Blended and Gridded High Resolution Global Sea Surface Windspeed and Climatology from Multiple Satellites: 1987–Present*. American Meteorological Society.

Zhang, J., Benoit, M., Kimmoun, O., Chabchoub, A., Hsu, H.C., 2019. *Statistics of extreme waves in coastal waters: Large scale experiments and advanced numerical simulations*. Fluids 4.